RESEARCH ARTICLE

CLIMATE CHANGE

Multiplatform evaluation of global trends in wind speed and wave height

Ian R. Young[1]* and Agustinus Ribal[1,2]

In this study, global satellite data were analyzed to determine trends in oceanic wind speed and significant wave height over the 33-year period from 1985 to 2018. The analysis uses an extensive database obtained from 31 satellite missions comprising three types of instruments—altimeters, radiometers, and scatterometers. The analysis shows small increases in mean wind speed and significant wave height over this period, with larger increases in extreme conditions (90th percentiles). The largest increases occur in the Southern Ocean. Confidence in the results is strengthened because the wind speed trends are confirmed by all three satellite systems. An extensive set of sensitivity analyses confirms that both the mean and 90th percentile trends are robust, with only small impacts caused by satellite calibration and sampling patterns.

Understanding the global wind and wave climate, and how it may be changing, is important for a variety of reasons. For example, ocean waves play a central role in defining the air-water boundary roughness (*1*) and thus affect the magnitude of fluxes of energy and CO_2 between the atmosphere and ocean. Also, breaking-wave setup can be an important component of total water level during storms (*2*), a factor made even more impactful by the sea level rise that is accompanying the warming of our planet. Therefore, estimates of future ocean wind and wave states, and whether extreme conditions are changing, are important elements of projections of total sea level.

A key aspect of making accurate projections of ocean winds and waves is understanding whether their characteristics have changed recently (i.e., in the past 30 years) and the mechanisms that may be driving such changes. To date, though, accurate determination of relatively small trends in measured records has proved problematic. Ocean buoys are the most obvious data source for long-term oceanic wind and wave observations. However, a number of studies (*3*) have indicated that changes in buoy hulls, instrumentation packages, and processing methods mean that the buoy dataset is not homogeneous and is generally unsuitable for long-term trend analysis. The satellite record, which provides global coverage, now spans 33 years (1985–2018) (*4*) and includes data from altimeters (which measure significant wave height and wind speed), radiometers (which measure wind speed), and scatterometers (which measure wind speed and direction). Initial applications of the satellite records (*5*) have proved promising, but the potential for bias in these records has raised doubts about the veracity of resulting trends. In particular, concerns have been raised about the consistency of calibration across multiple satellite platforms (*4*, *6*), the apparent differences in observed magnitudes of wind speed trends between altimeter and radiometer data (*7*), potential for under-sampling and fair-weather bias, and the validity of observations of extreme conditions (*8*, *9*).

Here we report on the analysis of an extensive satellite database consisting of 13 altimeter, 11 radiometer, and 7 scatterometer missions, spanning 33 years (1985–2018) [see supplementary materials section 1 (SM1) and fig. S1]. The dataset is analyzed to determine long-term global trends in wind speed and significant wave height. This analysis addresses many of the existing concerns about such satellite records. Specifically, we show consistent trends between altimeter and radiometer wind speed, we resolve apparent inconsistencies in the magnitudes of wind speed and significant wave height trends, and we demonstrate improved confidence in trend extraction for both mean values and higher-percentile extremes (i.e., 90th percentiles).

[1]Department of Infrastructure Engineering, University of Melbourne, Melbourne, Victoria, Australia. [2]Department of Mathematics, Faculty of Mathematics and Natural Sciences, Hasanuddin University, Makassar, Indonesia.
*Corresponding author. Email: ian.young@unimelb.edu.au

Datasets and processing

The primary dataset used in this analysis is a combined global altimeter record consisting of all 13 altimeters that have been in operation between 1985 and 2018 (see SM1 for details). Altimeters have the advantage of measuring both wind speed and significant wave height. Because these quantities are related, coincident measurement of both quantities adds to the physical interpretation of the results (see below). Two additional datasets are also considered—a radiometer dataset consisting of 11 radiometers operational from 1986 to 2013 and a scatterometer dataset consisting of 7 scatterometers operational from 1992 to 2018 (see SM1). These datasets are used to verify elements of the altimeter trends. All three datasets have been calibrated against National Data Buoy Center data, validated against an independent buoy dataset, and cross-validated against other satellites at crossover points (*4*). This cross-validation considers altimeter-altimeter, altimeter-radiometer, and altimeter-scatterometer crossovers. Further, the satellites are compared against aggregated buoy data to ensure that there are no spurious trends or discontinuities in the satellite data records (*4*, *6*). The accuracy of the altimeter, radiometer, and scatterometer data has been evaluated against buoys at both mean and higher percentiles (*4*, *9*). As such, the datasets represent an extensively calibrated and homogeneous multiplatform record.

We aggregated the data into 2°-by-2° bins to form stable statistics by ensuring sufficient observations in each bin (*5*). Monthly values for both wind speed, U_{10}, and significant wave height, H_s, were determined for each 2° bin (mean, mode, and 90th percentile). The linear trend over a variety of time periods was then determined as the Sen slope (*10*–*12*) for each of the statistics of mean, mode, and 90th percentile. Tests were also performed to determine whether the resulting trends are statistically significant, including accounting for serial dependence in the data (*5*, *10*–*14*) (SM2). Our analysis does not take into account the possible impact of long-duration (decadal) oscillations, which may affect the resulting trend values.

Results

Figure 1 shows the mean and 90th percentile altimeter trends in U_{10}. The corresponding mean and 90th percentile trends in H_s are shown in Fig. 2. In both cases, the trends span the period from 1985 to 2018. The mean wind speed (Fig. 1A) shows a broad region of increasing wind speeds across the Southern Ocean (approximately +2 cm/s per year). A similar band of increasing mean wind speed lies across the region south of the equator in both the Pacific and Atlantic oceans. This region is slightly smaller in magnitude than the Southern Ocean region. A less well-defined area of increasing mean winds (approximately +1 cm/s per year) exists across the North Atlantic. All these areas have statistically significant positive trends. Other areas of the world have a small positive trend or no clear trend at all. There are no significant regions of negative trend (decreasing mean wind speeds). The 90th percentile trend in U_{10} (Fig. 1B) shows similar spatial distributions to the mean wind speed trends, but the magnitudes are larger. The 90th percentile trend in U_{10} for the Southern Ocean is approximately +5 cm/s per year, and trends south of the equator in the Pacific and Atlantic oceans are approximately +2 to +3 cm/s per year. The region of increasing wind speed in the North Atlantic is much better defined for the 90th percentile, with trends of approximately +4 cm/s per year. Areas of positive trends are also apparent in the North Pacific and Indian oceans (approximately +2 cm/s per year). Again, all these regions of increasing 90th percentile wind speeds are statistically significant. The positive trends in wind speed over the Southern Ocean are consistent with model and anemometer data, indicating a strengthening of Southern Ocean westerlies in recent decades (*15*–*18*). Similarly, the positive trends in equatorial Pacific wind speeds are consistent with observations of increased trade winds in this region over the past two decades (*18*, *19*).

Figure 2 shows the corresponding trends in mean and 90th percentile H_s. Whereas the mean trend in U_{10} showed distinct regions of statistically significant positive trends across the Southern Hemisphere, Fig. 2A shows far less clear trends for mean significant wave height. There are areas of weak positive trends in the Southern Ocean south of the Pacific and Atlantic oceans (approximately +0.3 cm/year). However, south of the Indian Ocean there is no obvious indication of a trend. The trend is not clearly statistically significant in any of these areas. As for wind speed, the North Atlantic shows a weak positive trend (approximately +0.3 cm/year, not statistically significant). In contrast to wind speed, for which the North Pacific showed no clear trend, mean H_s in the North Pacific shows a distinct negative trend (approximately −0.5 cm/year, statistically significant). As with the wind speed, 90th percentile trends in H_s (Fig. 2B) are more positive than the mean values. There is a broad region of positive trend in the 90th percentile H_s across the Southern Ocean (approximately +1 cm/year) and in the North Atlantic (approximately +0.8 cm/year). For both regions, the 90th percentile trend in H_s is statistically significant. Whereas the mean trend in H_s in the North Pacific was negative, the 90th percentile shows a convoluted situation, with the northernmost parts displaying a positive trend that becomes more negative with increasingly southern latitudes (although trends in this region are not statistically significant).

The results depicted in Figs. 1 and 2 suggest that upper (90th) percentile trends are increasing faster than mean trends, which is consistent with previous limited observations (*5*). In addition, the mean wind speed seems to have positive trends for large areas of the world, which is not reflected in mean significant wave heights. Many of the world's oceans are dominated by remotely generated swell rather than by local wind sea (*20*, *21*). Therefore, an increase in mean local wind speed will not necessarily result in an increase in mean local significant wave height. However, at high latitudes (in both the Northern and Southern hemispheres), the waves are predominantly locally or regionally generated wind sea (*8*). As such, the results in Figs. 1 and 2 require further investigation.

Figure 3 shows trends in the mode [peak of the probability distribution function (PDF)] for wind speed and significant wave height. The trend in U_{10} mode (Fig. 3A) is similar in both magnitude and spatial distribution to the U_{10} mean (Fig. 1A). The spatial distribution of the trend in U_{10} mode values is slightly more uniform (globally positive) than the spatial distribution of the trend in mean values. In contrast, the trend in mode values of H_s (Fig. 3B) is globally negative, ranging from approximately −3 cm/year at high latitudes in both hemispheres to almost no trend at the equator. These differing results for the trend of the mean, mode, and 90th percentile suggest that changes have occurred in the shapes of the wind speed and significant wave height PDFs over the 33-year measurement period.

To better illustrate the changes in the respective PDFs, Fig. 4 shows the PDFs for wind speed and significant wave height averaged over the region 60°S to 46°S and 240°E to 270°E (Southern Ocean, west of South America). Data are shown for two periods, 1998–2000 and 2015–2017. This region was selected because it has a relatively uniform wind and wave climate, both spatially and temporally (over the course of multiple years). As such, we can average conditions there to produce statistically stable snapshots of the PDF changes. Other areas of the world do, however, also produce similar results. The wind speed PDF (Fig. 4A) broadens over this 17-year period and a small shift to higher values of the mode and mean occurs. As commonly reported, the shape of the wind speed PDF is relatively symmetric (*22*). The broadening of the wind speed PDF also results in a broader significant wave height PDF (Fig. 4B). The significant wave height PDF, however, is more strongly skewed, and the broadening of the PDF appears to result in a greater percentage of waves less than the peak of the PDF. This yields a decrease in the mode of the distribution and almost no change in the mean.

The reason for this behavior cannot be determined absolutely from the observed data, however, it is likely related to changes in the durations over which winds of various strengths blow. That is, at stronger wind speeds (values higher than the peak of the PDF), there may be an increase in wind speed, but if the duration of such winds is not sustained, it may result in no change (or even a reduction) in the significant wave height, as seen in Figs. 3B and 4B (see SM6).

Consistency analysis

Although the satellite data used in Figs. 1 to 4 were carefully calibrated against buoy data, issues such as satellite sampling pattern, the ability to accurately resolve extreme conditions, and geographical variations in quantities sensed can

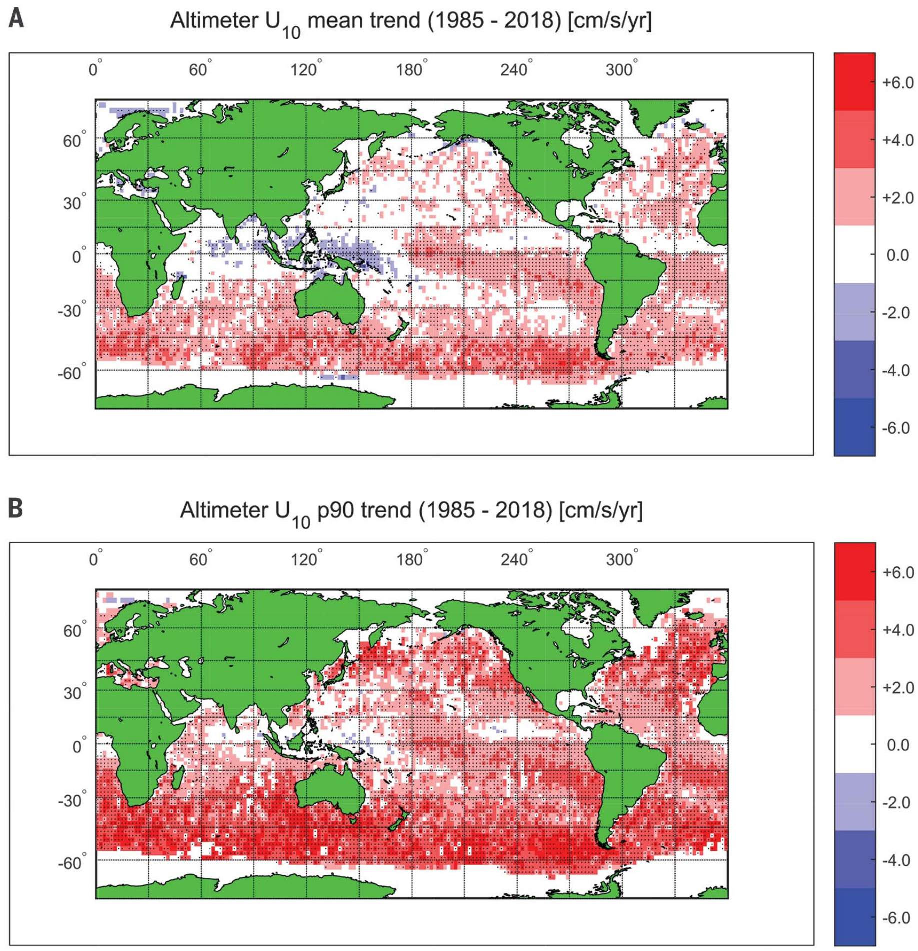

Fig. 1. Global trend in altimeter wind speed over the period 1985–2018. (**A**) Mean trend and (**B**) 90th percentile (p90) trend in altimeter U_{10}. Values that are statistically significant according to the Seasonal Kendall test are marked with a black dot.

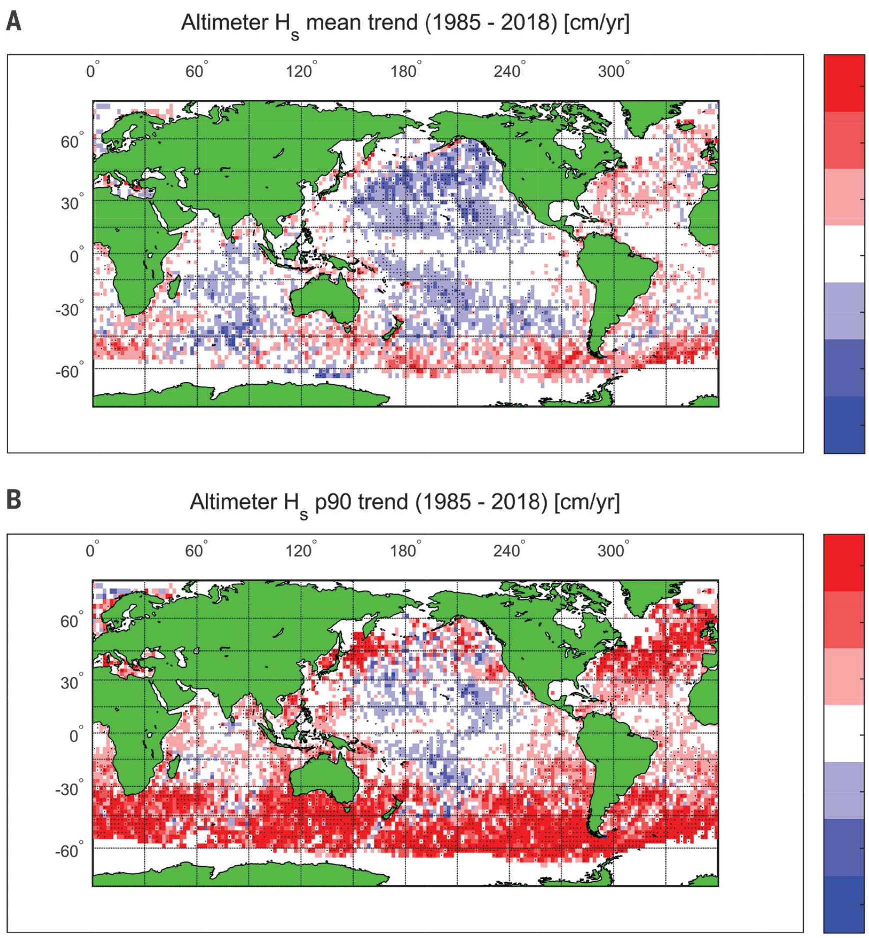

Fig. 2. Global trend in altimeter significant wave height over the period 1985–2018. (**A**) Mean trend and (**B**) 90th percentile trend in altimeter H_s. Values that are statistically significant according to the Seasonal Kendall test are marked with a black dot.

potentially affect trend estimates (*6*, *9*). To investigate potential bias caused by such issues, a range of detailed investigations were undertaken.

It has previously been reported that radiometer wind speed trends are considerably smaller than altimeter trends (*7*). This study's datasets provide an opportunity to test consistency across these two satellite systems. The physical mechanisms used by radiometers (brightness temperature) and altimeters (radar cross section) to sense wind speeds are quite different, as are the sampling patterns; radiometers measure 1400-km-wide swaths, altimeters sample along-track from their nadir. Figures S2A and S3A show altimeter mean wind speed trends for the periods 1985–2008 and 1985–2013, respectively. The comparable radiometer mean wind speed trends are shown in figs. S2B and S3B. The period from 1985 to 2008 is the same as previously investigated (*6*). The spatial distributions of the altimeter and radiometer mean wind speed trends are very similar. The radiometer results show smoother variations, as one would expect with a dataset ~20 times larger than that of the altimeter. The radiometer trends are also ~25% smaller than those of the altimeter. The longer time period (fig. S3) shows slightly smaller trends for both radiometer and altimeter data, most likely in response to multiyear variations altering the resulting linear trend. Importantly, both radiometer and altimeter data respond in the same manner, with the trend decreasing in magnitude for the longer period.

There are a number of potential processes that could account for the ~25% difference in the magnitude of the altimeter and radiometer mean trends. Changes in boundary layer shape associated with atmospheric stability can result in differences between altimeter and radiometer U_{10} (*8*). The results were recalculated using a full stability correction of the atmospheric boundary layer over the measurement period, with air and water temperatures obtained from monthly climatology. This analysis resulted in changes in the trend of <1%.

Diurnal variations in wind speed are known to occur (*23*, *24*), and the altimeter and radiometer missions take measurements at different times of day (generally in sun-synchronous orbits). On average, radiometer overpasses occur ~5 hours earlier than altimeter passes (see fig. S4A). In addition, the mean times of both altimeter and radiometer overflights have drifted earlier in the day over the 1985–2013 period (by ~6 hours) (see fig. S4B). An analysis of the impact of these timing issues on the resulting trends (SM4) shows that the differences are consistent with the observed 25% difference between altimeter and radiometer trends.

The altimeter sampling pattern is such that a single satellite will repeat its ground track only every 3 to 10 days, depending on the details of the satellite orbit (*6*). As a result, it is possible for a single satellite to under-sample geographically small meteorological systems. Such impacts decrease as the length of the sampling period increases. However, we use mean and 90th percentile values, determined on a monthly basis, to calculate trends (monthly Mann-Kendall approach, see SM2). If these monthly statistics are not accurately determined, this could lead to errors in the resulting trends. To test the sensitivity of trends determined from monthly statistics, we also performed trend estimates using annual values (see figs. S6 and S7). Annual trend estimates present a range of additional issues. For instance, with only 33 annual values, confidence limits on the trend estimates increase. A missing month in the data can greatly bias the annual estimate, meaning the actual time series is often reduced to as few as 20 values. Despite these limitations, figs. S6 and S7 show trends that are comparable to those determined from monthly values (Figs. 1 and 2). The mean trends are in particularly good agreement, whereas the 90th percentile trends obtained with the annual values are slightly smaller than the corresponding trends obtained from monthly values. Despite the increased noise of the annual trends, the spatial distributions of the 90th percentile trends are consistent between monthly and annual estimates.

A further series of tests were undertaken by randomly decimating the data by a factor of 1 to 5 (i.e., a factor of 5 means only one-fifth of the data are retained). The results for a location at 50°S, 200°E (Southern Ocean) are shown in table S1. Values for the mean and 90th percentile trends are shown for both wind speed and significant wave height. As the level of decimation increases, the trend estimates become less stable. For decimation factors >3, errors as large as 40% in the value of the 90th percentile trends occur. However, in no case does the sign of the trend change.

Another concern regarding the estimates of the trends of the upper percentiles (e.g., the 90th percentile) is the fact that the number of operational satellites has increased over time (see fig. S1) (*6*); with more satellites, it is likely that more storms will be sampled by the altimeters. Due to the potential under-sampling caused by the earlier sparseness of altimeter passes, it is possible that a spurious trend results for the 90th percentile values. A series of tests were performed in which specific satellites were removed to yield an approximately uniform sampling rate over time. These tests indicated that changes in the number of satellite observations over time has

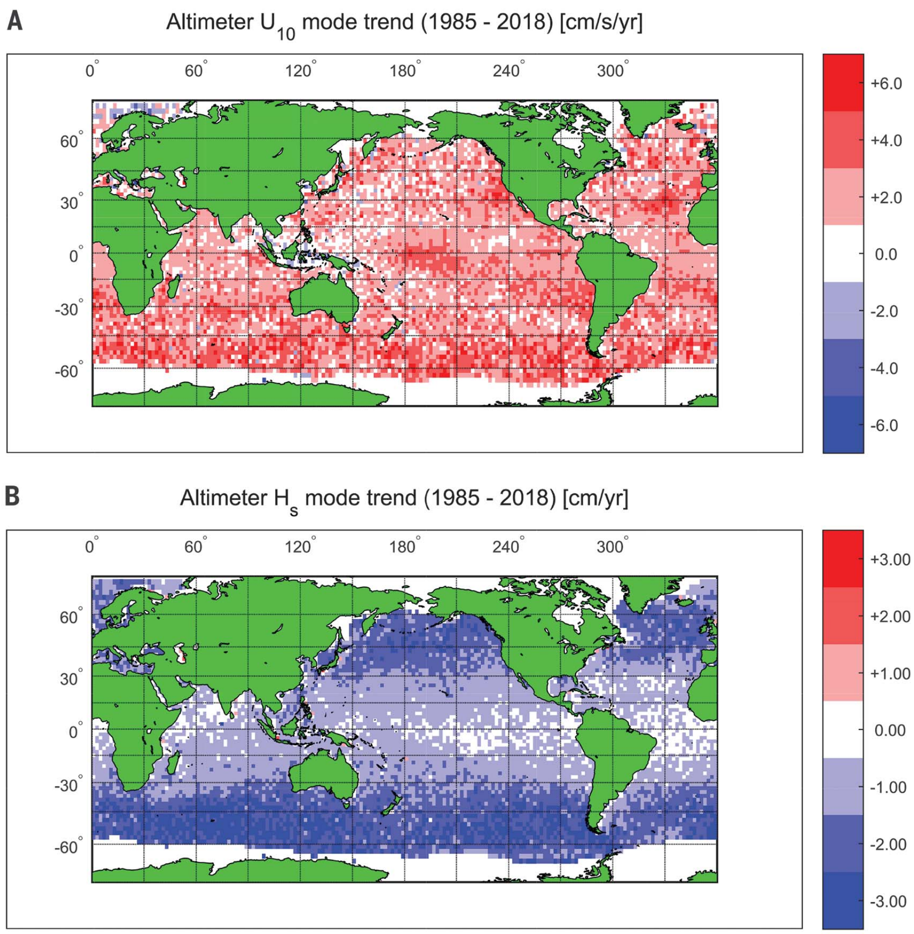

Fig. 3. Global trends in the altimeter wind speed and significant wave height mode over the period 1985–2018. (**A**) U_{10} mode trend and (**B**) H_s mode trend.

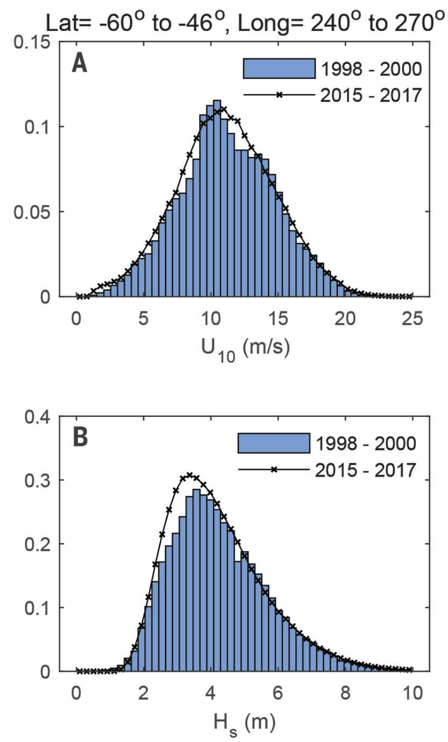

Fig. 4. Probability distribution functions for the region bounded by 60°S to 46°S and 240°E to 270°E. Data for the periods 1998–2000 (blue bars) and 2015–2017 (solid black line) for (**A**) U_{10} and (**B**) H_s.

had only a small impact on both the mean and 90th percentile trends (SM5.3).

Although altimeters have the potential for spurious extreme-value (90th percentile) trends due to their relatively low sampling rates and changes in the number of satellites over time, neither radiometers nor scatterometers have this limitation. Because of the wide area over which they both measure, radiometers and scatterometers will image a given location twice per day, even with only a single satellite in orbit. As such, they should provide a strong validation of the 90th percentile trends observed by the altimeters. Unfortunately, radiometers cannot measure through heavy rain and thus have a fair-weather bias, which limits their ability to accurately determine higher percentile wind speeds (*9*). Scatterometers, however, do not have this limitation, and fig. S9 shows their mean and 90th percentile trends. Although there are some regional differences between the scatterometer results and those of altimeters and radiometers (see SM7), both mean and 90th percentile trends are positive and of consistent magnitude to those of the other instruments. Importantly, the scatterometer trend for the 90th percentile wind speed is greater than the mean wind speed, which is consistent with the altimeter trend.

Outlook

Our analysis of three independent, long-duration satellite datasets shows that there have been statistically significant positive trends in mean wind speed, and even stronger trends in extreme (90th percentile) values over this period. There are strong regional variations, with the area of most significant increase in mean wind speed being the Southern Ocean, with weaker positive trends in the equatorial Pacific and North Atlantic oceans. These changes are accompanied by a broadening of the PDF of wind speed, resulting in an increase in the mean, mode, and upper percentiles. The increase in percentage of relatively light winds resulting from the broadening of the PDF causes strong growth in the percentage of smaller waves. In contrast, the increase in percentage of stronger winds results in only a small increase in larger waves, probably owing to changes in the duration of these stronger winds. As a result, there are only relatively small changes in global mean significant wave heights, most of which are not statistically significant, and a global decrease in values of the mode of the significant wave height PDF. The Southern Ocean shows regions of statistically significant increase in mean significant wave height and the Pacific Ocean shows regions of statistically significant small decreases in mean significant wave height. The increase in extreme winds is matched by an increase in extreme waves (90th percentile). The regional distribution of trends for the 90th percentile wind speed shows statistically significant increases in most areas. In contrast, increases in 90th percentile waves are confined to the Southern and North Atlantic oceans. Confidence in the results is gained by the fact that similar mean wind speed trends are apparent in all satellite measurements—altimeter, radiometer, and scatterometer. An extensive analysis of sampling patterns, together with validation from scatterometer extreme winds, also provides confidence that the 90th percentile trends for both wind speed and significant wave height observed by the altimeter are robust.

REFERENCES AND NOTES

1. M. A. Donelan, W. M. Drennan, K. B. Katsaros, *J. Phys. Oceanogr.* **27**, 2087–2099 (1997).
2. L. Mentaschi, M. I. Vousdoukas, E. Voukouvalas, A. Dosio, L. Feyen, *Geophys. Res. Lett.* **44**, 2416–2426 (2017).
3. J. Gemmrich, B. Thomas, R. Bouchard, *Geophys. Res. Lett.* **38**, L22601 (2011).
4. I. R. Young, E. Sanina, A. V. Babanin, *J. Atmos. Ocean. Technol.* **34**, 1285–1306 (2017).
5. I. R. Young, S. Zieger, A. V. Babanin, *Science* **332**, 451–455 (2011).

6. S. Zieger, J. Vinoth, I. R. Young, *J. Atmos. Ocean. Technol.* **26**, 2549–2564 (2009).
7. F. J. Wentz, L. Ricciardulli, *Science* **334**, 905 (2011).
8. I. R. Young, M. A. Donelan, *Remote Sens. Environ.* **215**, 228–241 (2018).
9. A. Takbash, I. R. Young, O. Breivik, *J. Clim.* **32**, 109–126 (2019).
10. R. M. Hirsch, J. R. Slack, R. A. Smith, *Water Resour. Res.* **18**, 107–121 (1982).
11. R. M. Hirsch, J. R. Slack, *Water Resour. Res.* **20**, 727–732 (1984).
12. P. K. Sen, *J. Am. Stat. Assoc.* **63**, 1379–1389 (1968).
13. M. Kendall, *Rank Correlation Methods* (Griffin, 1955).
14. H. B. Mann, *Econometrica* **13**, 245–259 (1945).
15. L. Menviel *et al*., *Nat. Commun.* **9**, 2503 (2018).
16. K. M. Saunders *et al*., *Nat. Geosci.* **11**, 650–655 (2018).
17. L. B. Hande, S. T. Siems, M. J. Manton, *Geophys. Res. Lett.* **39**, L11802 (2012).
18. J. Wohland, N.-E. Omrani, D. Witthaut, N. S. Keenlyside, *J. Geophys. Res. Atmos.* **124**, 1931–1940 (2019).
19. M. H. England *et al*., *Nat. Clim. Chang.* **4**, 222–227 (2014).
20. A. Semedo, K. Suselj, A. Rutgersson, A. Sterl, *J. Clim.* **24**, 1461–1479 (2011).
21. I. R. Young, *Int. J. Climatol.* **19**, 931–950 (1999).
22. S. P. Neill, M. R. Hashemi, *Fundamentals of Ocean Renewable Energy* (Academic Press, 2018).
23. C. Deser, C. A. Smith, *J. Clim.* **11**, 1730–1748 (1998).
24. S. Kako, A. Okuro, M. Kubota, *J. Atmos. Ocean. Technol.* **34**, 631–642 (2017).

ACKNOWLEDGMENTS

Funding: The authors gratefully acknowledge the support of the Australian Research Council through grants DP130100215 and DP160100738 and the Integrated Marine Observing System (IMOS), which is part of the National Collaborative Research Infrastructure Scheme of the Australian Government. **Author contributions:** I.R.Y. conceived of the project and conducted most of the analysis. A.R. calibrated and validated the most recent altimeter datasets (2013–2018) and the scatterometer data. Both authors wrote the paper. **Competing interests:** The authors declare no competing interests. **Data and materials availability:** The raw datasets used in the study were supplied by Globwave (http://globwave.ifremer.fr/), RADS (http://rads.tudelft.nl/rads/rads.shtml), NSOAS (www.nsoas.org.cn/) (altimeter data), and Remote Sensing Systems (www.remss.com/) (radiometer data). The processed altimeter records are available through the Australian Ocean Data Network (AODN) (https://portal.aodn.org.au/). The scatterometer data were sourced from PODAAC (https://podaac.jpl.nasa.gov/), EUMETSAT (http://archive.eumetsat.int), and ESA (https://earth.esa.int).

SUPPLEMENTARY MATERIALS

science.sciencemag.org/content/364/6440/548/suppl/DC1
Materials and Methods
Supplementary Text
Figs. S1 to S10
Table S1
References (*25*–*34*)

4 November 2018; accepted 10 April 2019
Published online 25 April 2019
10.1126/science.aav9527

Science

Multiplatform evaluation of global trends in wind speed and wave height

Ian R. Young and Agustinus Ribal

Science **364** (6440), 548-552.
DOI: 10.1126/science.aav9527originally published online April 25, 2019

Ocean winds blowing harder

Two frequently asked questions about how climate warming will affect the environment are whether windiness might change and what effects that might have on ocean waves. Young and Ribal analyzed global satellite data over the period from 1985 to 2018 to determine if there are any trends in oceanic wind speed and wave height. They found small increases in both quantities, with the strongest increases in extreme conditions and in the Southern Ocean. These findings are important for understanding air-sea exchange of energy and carbon dioxide and for projecting sea levels during storms.

Science, this issue p. 548